Spectral Density Matrices Used to Characterize Vibration Environments

Luke A. Martin and **Shawn P. Schneider**, Naval Surface Warfare Center – Dahlgren Division, Dahlgren, Virginia

In recent years, new technologies in vibration laboratory test equipment have allowed for successful recreation of real-world, multiple-degree-of-freedom (MDOF) vibration environments. However, a knowledge vacuum currently exists between MDOF laboratory capabilities and common laboratory test specifications often defined in MIL-STDs, product specifications, or other requirement documents. This knowledge vacuum is due to the fact that MDOF tests require more information about the vibration environment than single-degree-of-freedom (SDOF) test specifications traditionally provided. The new information required is best explained by examining the spectral density matrix (SDM) and understanding how the SDM applies for SDOF and MDOF tests. The SDM is the complete test definition for an environmental vibration test. The size of the SDM determines the maximum number of spatial degrees of freedom (DOF) that can be defined. Typically, the size of the SDM available and the laboratory setup will determine the appropriate control strategy for the vibration test. The SDM can be easily collapsed to define tests of lesser DOF. For SDOF tests, the SDM collapses to a single, power spectral density (PSD). The nature of SDMs used to characterize vibration environments are discussed, along with insight into cross spectral density (CSD) definitions and a reasonable approach for defining acceptable tolerances based on the actual environmental data. This article is intended to serve as a pragmatic approach to understanding PSDs and CSDs used to characterize MDOF environments and used to define MDOF tests.

Three primary elements are required to conduct MDOF testing. The MDOF testing Venn diagram (Figure 1) illustrates these three elements, which are: shaker systems, control systems, and environmental definitions.

The term shaker systems is used and refers to the physical actuation device and all the support equipment to include, but not limited to: modern pad-bearing design, spherical couplings, linear bearings, honeycomb fixtures, general fixtures, and slip tables. Advances in shaker system technology have made the mechanical realization of MDOF vibration environments possible.

The term vibration controllers is meant to define the hardware and software used to acquire an analog signal from a vibration test, digitally process the signal, compare results to a desired test reference, and output an analog signal to the shaker system to perform closed-loop control. The MDOF closed-loop control problem is much more complex, both mathematically and figuratively, than the SDOF closed-loop control problem. The required digital signal processing speed, advanced control algorithms, analog-to-digital converters, and relative cost of modern vibration controllers have allowed vibration laboratories to mathematically realize the closed-loop control problem required to conduct a MDOF vibration test.

Finally, the third element necessary for conducting MDOF testing is an appropriate environmental definition. The focus of this article will be on sharing experiences based on analyzing MDOF environmental vibration data from actual field environments. The intent here is to share insight into some of the mathematical considerations that should be given to the MDOF test definition problem and insight into the nature of field-measured SDMs. Finally, a discussion on test tolerances is included, because we believe a departure from the conventional SDOF thought process is required to arrive at reasonable test tolerances for MDOF tests. The traditional SDOF tolerances were likely derived from a lack of information about the environment and from knowledge of the
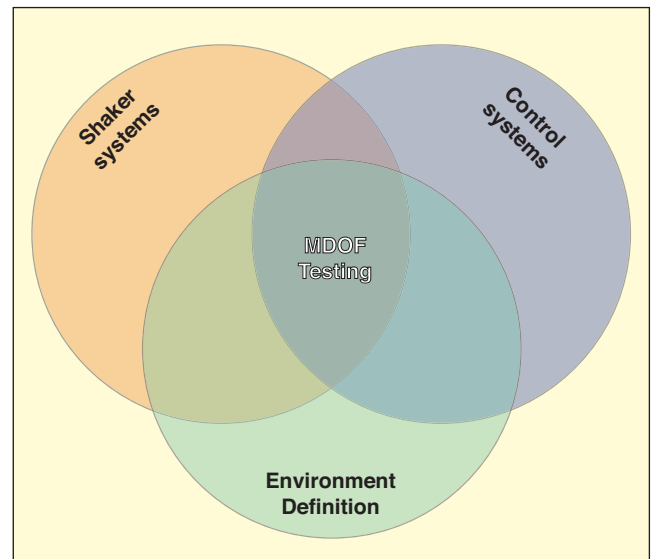
Figure 1. Venn diagram.

lab equipment's performance at the time adopted into the military standards. However, the suggested path forward for MDOF tolerances is a departure from standard practice and for good reason, as will be explained.

The vibration data presented were measured on a commonly known military aircraft and represents two flights, each approximately 8 hours in duration.

Spectral Density Matrix Overview

This article intentionally approaches the SDM discussion from an informal point of view. More formal treatment of the mathematics can be found in References 1 and 2. The objective here is to discuss the nature of the SDM based on observations made in reviewing and analyzing field-measured data in an attempt to bridge the gap between those familiar with SDOF testing but have limited experience in MDOF testing. Currently, the literature is insufficient regarding the nature of actual SDMs based on field-measured data.

Introduction to Spectral Density Matrix. The SDM is a three-dimensional matrix (row, column, and depth). This paper focuses on SDMs whose: depth is frequency (Fourier domain), diagonal terms are PSDs, and nondiagonal terms are CSDs. Again, the PSDs and CSDs are functions of frequency as commonly treated in vibration laboratories. The SDM is derived from environmental surveys, where more than one sensor reading is available to describe the environment.

An important note is that the data acquisition system used to measure the sensor data should be phase locked so that no time delay is introduced between measurement channels by the act of digitizing. Ideally, a zero-phase tolerance is desired across all channels so that the samples across channels have the same time step. In practice, multiplexed analog-to-digital convertors are only recommended if the time skew between samples from channel to channel is known and very small. In such a case, the phase error as a function of frequency can then be estimated for the system. A full discussion on phase error is beyond the scope of this article but is an instrumentation detail that requires consideration when creating a SDM from a vibration survey.

Physical Meaning of Spectral Density Matrix. The predominate sensor used for vibration tests and surveys is the accelerometer. Therefore, this discussion will be limited to acceleration when
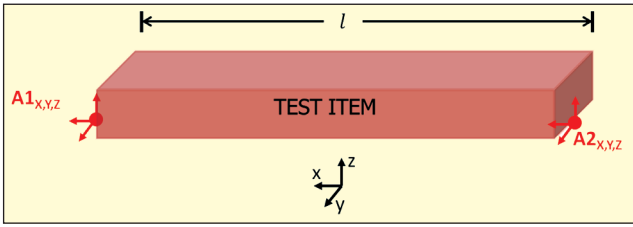
Figure 2. Vibration survey accelerometer placement.

discussing PSDs and CSDs.

To give insight into the physical meaning of an SDM, a fictitious test item will be considered with two triaxial accelerometers affixed to the bed or floor upon which the test item rests. The two triaxial accelerometers are placed on the bed or floor at a distance, l, apart as illustrated in Figure 2. The data measured by the two accelerometers can be used to construct an SDM. In practice, additional accelerometers should be used to improve the observability of structural modes. However, large SDMs are difficult to illustrate on 8.5 × 11-inch paper, so the six measurement channel case was investigated here.

The raw time domain data measured during the vibration survey depicted in Figure 2 can be represented in Equation 1. $DATA_{SURVEY}$ represents a 6×1×n matrix:

$$DATA_{SURVEY}(t) \begin{bmatrix} A1_x(t) \\ A1_y(t) \\ A1_z(t) \\ A2_x(t) \\ A2_y(t) \\ A2_z(t) \end{bmatrix} \quad (1)$$

The Fourier domain representation of a time domain accelerometer signal at location 1 in direction X is given in Equation 2:

$$A1_x(f) = fft\left(A1_x(t)\right) \quad (2)$$

The SDM is then computed by multiplying the acceleration column vector by its conjugate transpose as shown in equation (3):

$$SDM(f) = \begin{bmatrix} A1_X(f) \\ A1_Y(f) \\ A1Z(f) \\ A2_X(f) \\ A2_Y(f) \\ A2_Z(f) \end{bmatrix} \begin{bmatrix} A1_X{}^*(f) & A1_Y{}^*(f) & A1_Z{}^*(f) & A2_X{}^*(f) & A2_Y{}^*(f) & A2_Z{}^*(f) \end{bmatrix} = \quad (3)$$

$$\begin{bmatrix} A1_X{}^2(f) & A1_X(f)A1_Y{}^*(f) & A1_X(f)A1_Z{}^*(f) & A1_X(f)A2_X{}^*(f) & A1_X(f)A2_Y{}^*(f) & A1_X(f)A2_Z{}^*(f) \\ A1_Y(f)A1_X{}^*(f) & A1_Y{}^2(f) & A1_Y(f)A1_Z{}^*(f) & A1_Y(f)A2_X{}^*(f) & A1_Y(f)A2_Y{}^*(f) & A1_Y(f)A2_Z{}^*(f) \\ A1_Z(f)A1_X{}^*(f) & A1_Z(f)A1_Y{}^*(f) & A1_Z{}^2(f) & A1_Z(f)A2_X{}^*(f) & A1_Z(f)A2_Y{}^*(f) & A1_Z(f)A2_Z{}^*(f) \\ A2_X(f)A1_X{}^*(f) & A2_X(f)A1_Y{}^*(f) & A2_X(f)A1_X{}^*(f) & A2_X{}^2(f) & A2_X(f)A2_Y{}^*(f) & A2_X(f)A2_Z{}^*(f) \\ A2_Y(f)A1_X{}^*(f) & A2_Y(f)A1_Y{}^*(f) & A2_Y(f)A1_Z{}^*(f) & A2_Y(f)A2_X{}^*(f) & A2_Y{}^2(f) & A2_X(f)A2_Z{}^*(f) \\ A2_Z(f)A1_X{}^*(f) & A2_Z(f)A1_Y{}^*(f) & A2_Z(f)A1_Z{}^*(f) & A2_Z(f)A2_X{}^*(f) & A2_Z(f)A2_Y{}^*(f) & A2_Z{}^2(f) \end{bmatrix}$$

The notation $A1_X{}^*(f)$ is used to represent the complex conjugate of $A1_X(f)$. When Eq. 3 is normalized by multiplying both sides by 1/Δf, the autospectrums that are found along the diagonal assume the form of power spectrum densities (PSDs). A recommended sanity check is to compute the area under the spectral density function and compare to the root-mean-square of the original time signal to ensure they are equal.[1]

The SDM will contain off-diagonal terms, which are referred to as the CSD terms. The CSD terms contain the relational information between the two measurements. From a modal analysis perspective, the CSDs can be viewed as the phase and coherence between respective signals. The CSDs found below the diagonal are the complex conjugates of the CSDs found mirrored above the diagonal.

The 6×6 SDM given in Eq. 3 representing data surveyed from Figure 2 can be divided into four parts as shown in Equation 4. In Eq. 4, the upper left 3×3 matrix ($ULM_{3\times3}$) contains three PSDs along the diagonal and three unique cross-spectral densities on the off-diagonals. Note the upper triangular terms are the complex conjugates of the lower triangular terms in $ULM_{3\times3}$. $ULM_{3\times3}$ contains only acceleration data from accelerometer 1 ($A1$). Notice the lower right 3×3 matrix ($LRM_{3\times3}$) contains the same characteristics as $ULM_{3\times3}$, except the data are from accelerometer 2 ($A2$). The CSDs in $ULM_{3\times3}$ and $LRM_{3\times3}$ contain the cross-axis information between accelerometers located, typically, on the same triaxial accelerometer

Globally, relative to the larger structure under survey, these accelerometers $A1_X$, $A1_Y$, and $A1_Z$ can be thought about as occupying the same point in space or approximate the same point in space. Thus, the CSD relationships between these accelerometers pertain more to the local dynamics of the measurement location and less to the global structural dynamics of the environment. Therefore, in a hierarchy of CSD importance for future laboratory testing, $ULM_{3\times3}$ and $LRM_{3\times3}$ would be weighted lower than $URM_{3\times3}$ and $LLM_{3\times3}$. In the event that SDM correction needs to occur, these CSDs are of lower importance and should be the first CSDs to be reduced. A technique for adjusting CSDs is defined in Reference 3. Adjusting CSDs is often necessary after analysis of a cloud plot, particularly when statistics are applied to the distribution of ensembles to arrive at a representative test definition. The adjustments are made to ensure the resulting SDM is Hermitian positive-definite.

In Eq. 4, the lower left 3×3 matrix ($LLM_{3\times3}$) and the upper right 3×3 matrix ($URM_{3\times3}$) contain solely CSDs. The $LLM_{3\times3}$ is the complex conjugate of the $URM_{3\times3}$. Therefore, the discussion will be limited to the $URM_{3\times3}$, yet applies to both matrices. The $URM_{3\times3}$ represents CSDs between accelerometers $A1$ and $A2$. These CSDs contain the phase and coherence information between $A1$ and $A2$, which are spatially some distance apart.

In general, the CSDs from different accelerometers measuring in the same axes should be weighted more in a hierarchy of CSDs important for control of a future laboratory test. For MDOF laboratory vibration tests, a hierarchy of CSDs should be established for the in-service measured data. When the MDOF vibration specification is determined and brought to the laboratory for testing, the SDM adjustments can be made using the hierarchy established, as described in References 3 and 4. The ability to adjust particular CSDs is the primary advantage of the Monte Carlo approach taken in Reference 3 and 4 versus the eigenvalue or Cholesky correction approach recommended in Reference 2.

The Hermitian-positive definite requirement on the SDM is required for laboratory MDOF vibration controllers to conduct the test. The SDM correction, using a Monte Carlo approach, allows for particular CSDs to be targeted, while the
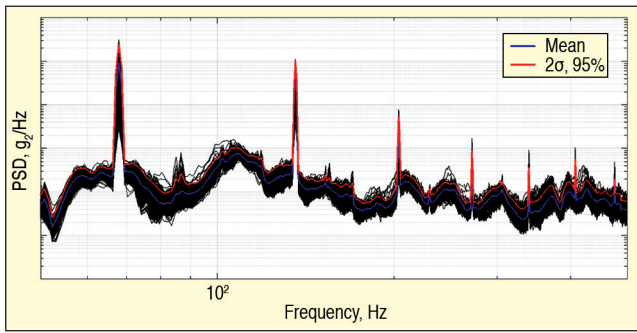
$$SDM(f) = \qquad\qquad ULM_{3X3} \qquad\qquad\qquad\qquad\qquad\qquad\qquad ULM_{3X3} \qquad (4)$$

$$\begin{bmatrix} A1_X{}^2(f) & A1_X(f)A1_Y{}^*(f) & A1_X(f)A1_Z{}^*(f) & A1_X(f)A2_X{}^*(f) & A1_X(f)A2_Y{}^*(f) & A1_X(f)A2_Z{}^*(f) \\ A1_Y(f)A1_X{}^*(f) & A1_Y{}^2(f) & A1_Y(f)A1_Z{}^*(f) & A1_Y(f)A2_X{}^*(f) & A1_Y(f)A2_Y{}^*(f) & A1_Y(f)A2_Z{}^*(f) \\ A1_Z(f)A1_X{}^*(f) & A1_Z(f)A1_Y{}^*(f) & A1_Z{}^2(f) & A1_Z(f)A2_X{}^*(f) & A1_Z(f)A2_Y{}^*(f) & A1_Z(f)A2_Z{}^*(f) \\ A2_X(f)A1_X{}^*(f) & A2_X(f)A1_Y{}^*(f) & A2_X(f)A1_X{}^*(f) & A2_X{}^2(f) & A2_X(f)A2_Y{}^*(f) & A2_X(f)A2_Z{}^*(f) \\ A2_Y(f)A1_X{}^*(f) & A2_Y(f)A1_Y{}^*(f) & A2_Y(f)A1_Z{}^*(f) & A2_Y(f)A2_X{}^*(f) & A2_Y{}^2(f) & A2_X(f)A2_Z{}^*(f) \\ A2_Z(f)A1_X{}^*(f) & A2_Z(f)A1_Y{}^*(f) & A2_Z(f)A1_Z{}^*(f) & A2_Z(f)A2_X{}^*(f) & A2_Z(f)A2_Y{}^*(f) & A2_Z{}^2(f) \end{bmatrix}$$

$$\qquad\qquad\qquad LLM_{3X3} \qquad\qquad\qquad\qquad\qquad\qquad\qquad\qquad\qquad LRM_{3X3}$$

Figure 3. Power spectral density cloud plot from 16 hours of vibration measurements.

eigenvalue and Cholesky approaches do not allow for particular CSDs to be targeted for adjustment. Therefore, the Monte Carlo approach can be considered a more localized approach with respect to the CSDs, in comparison to the eigenvalue or Cholesky approaches that tend to be a global correction of the SDM.

In Eq. 4, the recommended control emphasis should be placed on $A1_X(f)A2_X{}^*(f)$, $A1_Y(f)A2_Y{}^*(f)$, and $A1_Z(f)A2_Z{}^*(f)$. Notice, these are the diagonals of the $URM_{3\times3}$. In Figure 2, we can see that $A1_X$ and $A2_X$ represent axial dynamics. $A1_Y$ and $A2_Y$ will yield information pertaining to yaw. Finally, $A1_Z$ and $A2_Z$ will yield information pertaining to pitch.

SDOF and MDOF Considerations with a Discussion on Tolerances. The SDOF in-service measurement and SDOF laboratory test is the special case of an SDM with only one PSD and no cross spectrums. In the SDOF laboratory test, no cross spectrums exist from the in-service condition and are also not required to conduct a vibration test. Therefore, the SDM for a SDOF test is a single PSD.

Interestingly enough, SDOF laboratory tests have been conducted for years using average or maximum-control strategies with multiple-control accelerometers. In SDOF tests employing these type of control strategies, little attention has been given to the cross spectrum between the control accelerometers from a goodness-of-test perspective. The current MIL-STDs give little insight into suitable cross-spectrum acceptance between control

accelerometers. This has led to test fixture performance and location of the control accelerometers to be determined and evaluated locally at the test laboratory.

Given this lack of universal knowledge and agreement amongst test laboratories, two schools of thought have prevailed with regard to acceptable cross spectrums for control. The first approach is to simply design fixtures to be as rigid as possible with the intent of ensuring no flexible modes exist in the testing bandwidth of interest or to minimize flexible modes in the testing bandwidth, since the former is often unachievable. This approach is straightforward and may seem like the only logical approach. Essentially, the test laboratory is placing a similar requirement onto the test fixture as the community often places onto the shaker armature and slip table.

The second approach is to design fixtures to match the mechanical impedance of the test item's in-service condition. The second approach requires knowledge about the in-service condition, which often a test laboratory does not know but we think should strive to understand. The mechanical impedance refers to the actual in-service boundary conditions along with the test item's mass, stiffness, and damping properties. Reference 5 highlights the importance of structural interaction between a test item and the support structure (fixture).

In essence, Ewins[5] demonstrates the limitations of an SDOF test when the laboratory boundary conditions differ from the in-service boundary conditions. Additionally, he also demonstrates that when the in-service boundary conditions are properly approximated in the laboratory and more than one degree of freedom is considered, a more acceptable match to the in-service vibration environment can be made during a qualification test.

In traditional SDOF vibration test definitions, a single PSD curve is defined and a tolerance of ±3 dB is assigned around the PSD curve. In some cases, a tolerance of ±6 dB could be used or some combination of the two tolerances. In fact, MIL-STD-810 generally suggests using ±3 dB up to a frequency of 500 Hz and ±6 dB above 500 Hz.

In modern MDOF vibration test definitions, multiple PSD curves define the environment. In addition, CSD definitions are required to understand the timing and causality between inputs. Reference 6 describes a technique for determining the global test error for
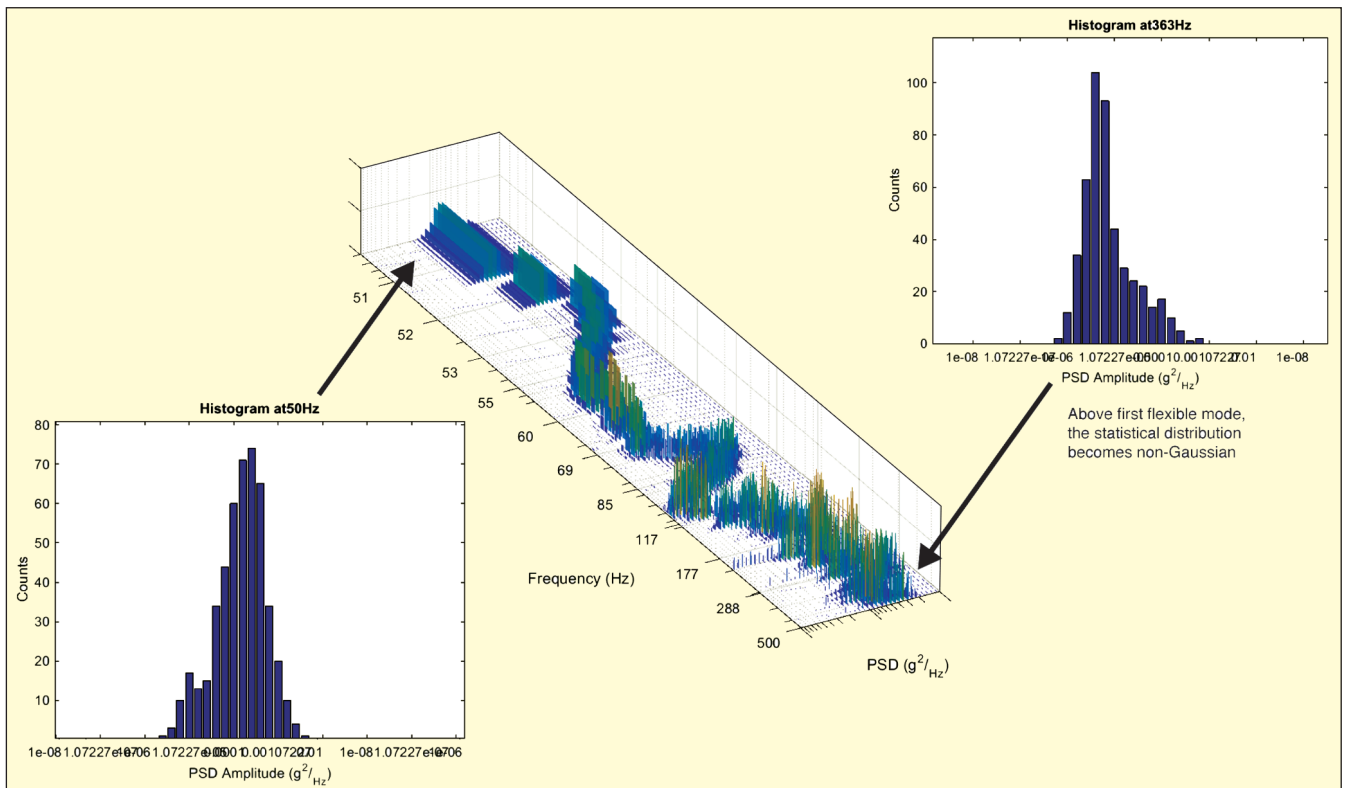

Figure 4. 3D histogram of PSD cloud plot as a function of frequency (center); Individual 2D histogram of the PSD at 50 Hz (left); individual 2D histogram of the PSD at 363 Hz (right).
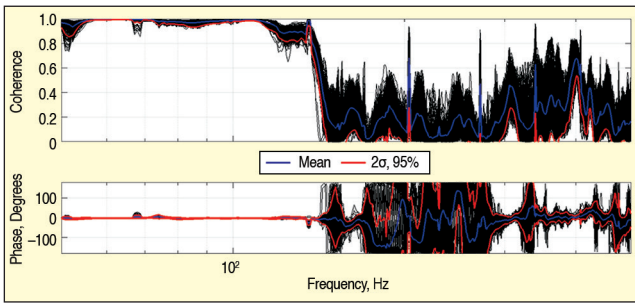
Figure 5. Cross-spectral density cloud plot from 16 hours of vibration measurements.

PSDs and how to associate it back to legacy tolerance definitions. Additionally, Reference 6 also describes methods for defining frequency-dependent tolerance bands and bandwidths for CSDs. This article describes additional and alternate considerations for defining the tolerances for both PSDs and CSDs.

The next two sections explore the nature of PSDs and CSDs. All the ensembles of data measured from a particular environment are plotted and reviewed; these ensembles are referred to as a cloud plot. The cloud plot provides a more complete environmental

definition and is recommended as the starting point for developing a vibration test definition, especially in the case of MDOF vibration testing.

The statistical nature of the PSDs and CSDs should drive the tolerance definitions for a particular test instead of arbitrary tolerance guidelines. In the case of CSDs, the use of control zones is recommended. A control zone is defined as a frequency band with a desired phase or coherence value and some desired tolerance about the defined reference. Frequency bands not defined as a control zone are bands that do not require a control tolerance definition; i.e., truly random phase and coherence where any value is acceptable.

Nature of In-Service Power Spectral Densities

The power spectral density (PSD) is a way to quantify the average power in a signal. In vibration testing practice, the terms auto spectral density (ASD) or acceleration spectral density (ASD) are also used by some authors interchangeably. The PSD is a useful tool for quantifying the average power in a steady-state random signal.

Figure 3 is a cloud plot, in black, representing 16 hours of vibration data. The mean value of all the individual PSDs is plotted in blue. Plotted in red is the mean plus two-sigma values.

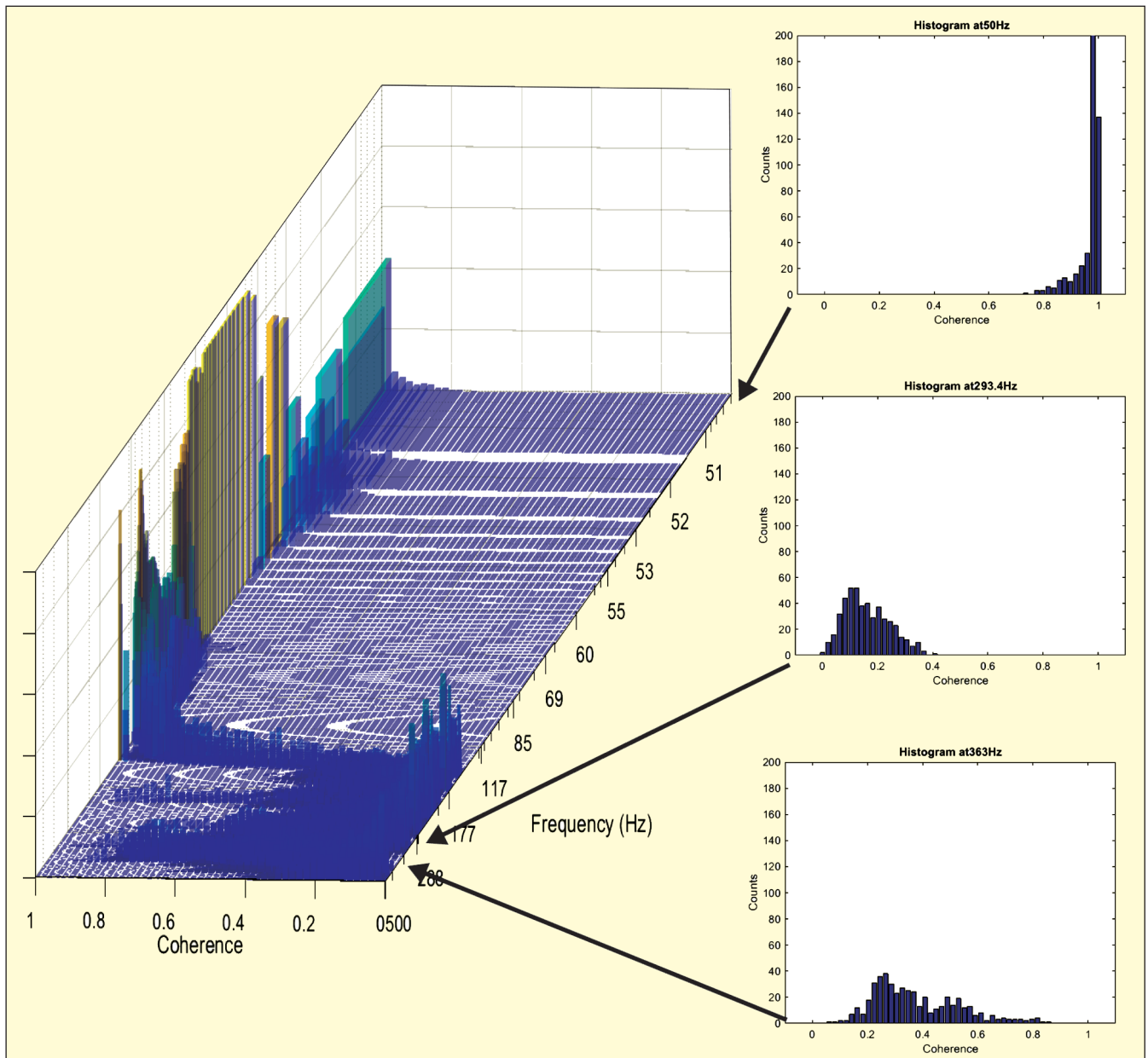A typical SDOF test definition would include the margin added,

Figure 6. 3D histogram of coherence cloud plot as a function of frequency (left); 2D histograms of coherence at 50 Hz, 293.4 Hz, and 363 Hz (right).
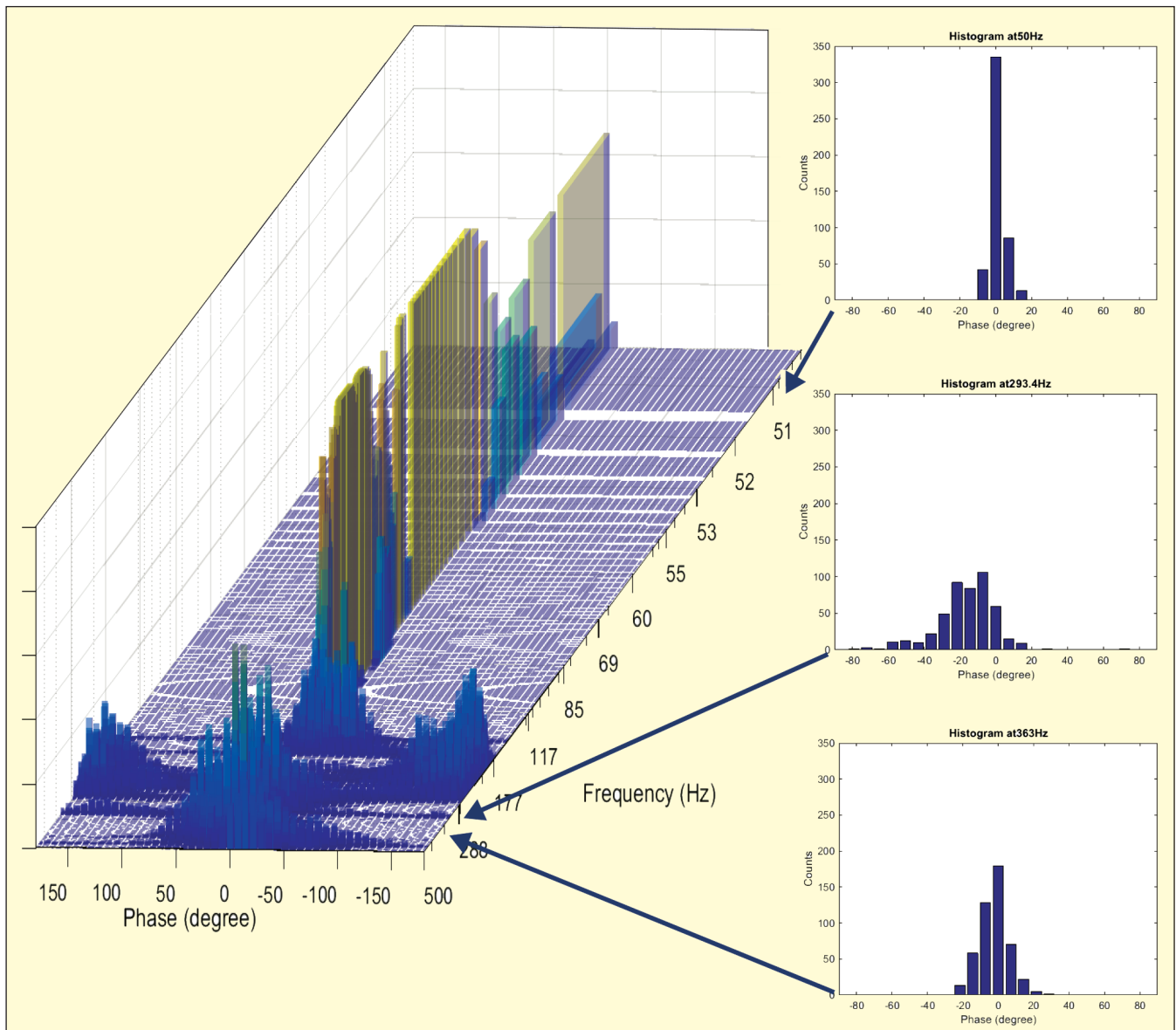
Figure 7. 3D histogram of phase cloud plot as a function of frequency (left); 2D histograms of phase at 50 Hz, 293.4 Hz, and 363 Hz (right).

in this case 2 sigma, to the mean curve. However, test specifications have often utilized the mean curve, 2-sigma curve or a maximum-measure curve depending on the application. Furthermore, time compression may be applied to one of these curves to determine a suitable test amplitude and duration. The time-compressed amplitudes and duration then would have traceability back to the in-service amplitudes and duration.

Little to no discussion regarding original cloud data and the statistical nature of cloud data was found in the literature. The remainder of this article studies the cloud data of PSDs and CSDs from a real-world measured environment in an effort to bridge the gap in literature. MDOF test definitions should be derived from data sets that contain a suitable quantity of data necessary to understand the actual environmental dynamics.

In the center of Figure 4, a three dimensional (3D) PSD histogram is reported. The plot is the combination of 2D histograms computed at each spectral line. The histogram appears to be Gaussian distributed at 50 Hz and up to 55 Hz. Above 55 Hz, the distribution changes from Gaussian, as illustrated by the 2D histogram plotted at 363 Hz on the right of Figure 4.

In studying the PSD in Figure 4, we observed that the Gaussian nature changes as a function of frequency. When the PSD in Figure 4 is studied with the coherence and phase in Figure 5, a structural dynamist may conclude that, above the first structural mode, the Gaussian nature of the PSD changes to a more random distribution or even a hybrid random-Gaussian distribution. Therefore,

knowing the actual nature of PSDs as a function of frequency is recommended when defining an MDOF environment and recreating this environment in a laboratory.

Nature of In-Service Cross-Spectral Densities

The CSD is used to study the relationship between two independent signals. A more formal approach and definition of CSDs can be found in References 1 and 7. The discussion here is again a pragmatic one from a structural dynamist's perspective.

The CSDs are used to report the "timing" (phase) and the "causality" (coherence) between two signals. Modern MDOF vibration control systems offer the ability to report CSDs in numerous ways, our preference is to report and study the phase and coherence. The phase and coherence allows for trained structural dynamists to leverage knowledge of modal analysis and operational modal analysis to interpret the CSD information.

Figure 5 shows a CSD cloud plot in phase and coherence for approximately 500 data sets. The mean and two sigma curves are shown analogous to the comparable PSD curves shown in Figure 3. The frequency band from 50 Hz to approximately 120 Hz illustrates how a structure exhibits rigid-body dynamics across this band. The rigid-body dynamics is indicated by the coherence being near unity and the phase near zero. This information can be used to understand spatially how the structure responds.

In Figure 6, a 3D coherence histogram is plotted, where the axes are frequency, coherence, and number of occurrences, or counts.

The 3D coherence plot is accompanied by a series of 2D coherence plots showing the histogram at frequencies of 50 Hz, 293.4 Hz, and 363 Hz, respectively.

In Figure 6, the first 2D histogram details the 50-Hz distribution. The coherence is near unity at 50 Hz. Again, a coherence value near unity with a phase at 0 degrees indicates the motion between these two measurement points can be described as rigid-body motion. The near unity coherence begins to change in the vicinity of 120 Hz.

The second 2D histogram is at 293.4 Hz. Comparing the 2D histograms at 50 Hz and 293.4 Hz, respectively, shows the distribution of the coherence is a function of frequency, and the shape of the distribution drastically changed. The frequency band above 120 Hz in the example is considered to be into the flexible region of the structure.

The third 2D histogram is at 363 Hz. Comparing all three 2D histograms shows that the distributions at three separate frequencies are distinctly different. At 363 Hz, the coherence value has the broadest spread, between 0.05 and 0.85. The greatest weighting would be given to the 0.2 to 0.3 range for the 363 Hz spectral line. From the viewpoint of developing a test specification, a much broader test tolerance would be acceptable at 363 Hz, when compared to 50 Hz and 293.4 Hz.

Figure 7 reports the 3D histogram of phase originally plotted two dimensionally as a cloud plot in Figure 5. The 3D histogram gives insight into how the statistical distribution of phase changes as a function of frequency. In Figure 7, the 3D phase plot is accompanied by a series of 2D coherence plots showing the histogram at frequencies of 50 Hz, 293.4 Hz, and 363 Hz, respectively.

In Figure 7, the first 2D histogram details the 50 Hz distribution. The phase is zero, or very near, at 50 Hz up to 120 Hz. Again, a phase value at or near zero with a coherence near unity indicates the motion between the two measurement locations used in computing the CSD can be described as rigid-body motion. The near-zero phase begins to change in the vicinity of 120 Hz.

Comparing the 2D histograms at 50 Hz and 293.4 Hz shows that the distribution's mean value has decreased in phase from approximately 0 degrees at 50 Hz to approximately 15 degrees, at 293.4 Hz. Additionally, the standard deviation, if fitting to a Gaussian distribution, increases from 50 to 293.4 Hz.

Comparing all three 2D histograms in Figure 7 shows the distributions at the three separate frequencies are distinctly different. At 363 Hz, the phase values have decreased in standard deviation when compared with the 293.4 Hz, 2D histogram. Additionally, the mean phase, which was near zero degrees at 50 Hz and near 15 degrees at 293.4 Hz, has moved back near zero degrees at 393 Hz.

Conclusions and Recommendations

This article presents a unique view of spectral density matrices by observing the statistical nature of numerous data ensembles, a cloud plot, as a function of frequency. When defining a MDOF test, a cloud-plot data review is recommended. In the cloud plot, a suitable quantity of data should be analyzed to ensure the environment's dynamic characteristics are captured. Additionally, the cloud-plot point of view can aid in developing reasonable test tolerances for both the PSDs and CSDs.

As an example, a SDM was computed using a fictitious, two-triaxial accelerometer setup. The resulting 6×6 SDM was then broken into four 3×3 submatrices with the physical meaning of the submatrices explained. A recommended hierarchy for the CSDs is discussed and strongly recommended when developing a laboratory control strategy or performing SDM adjustments. The in-service measured data captured in a cloud plot provides the necessary information for test laboratories to define and conduct MDOF tests. The CSDs pertaining to the global dynamics are recommended to be weighted heavier than the CSDs pertaining to local dynamics, such as three accelerometers located in the same sensor body. Additionally, a primer in modal analysis is recommended for analysts and laboratories who have experience in SDOF testing and wish to begin studying the full SDM for MDOF test definitions.

A need for Hermitian positive-definite SDMs was briefly reviewed. We give the background as to why and where to correct the SDMs, clarifying previous work in References 3 and 4. The previous works discuss *how* SDMs can be adjusted to meet the Hermitian positive-definite requirement. The Monte Carlo technique was discussed and is recommended, since the technique allows for CSDs to be placed in a hierarchy of importance based on contributions to global dynamics. The other advantage of the Monte Carlo technique is that the subset of CSDs causing the SDM to fail the Hermitian positive-definite check can be identified. Adjustments can be made to the CSDs causing the failed check, and the remaining CSDs are not disturbed.

A discussion on SDMs with respect to SDOF testing was given. The primary motivation of this discussion was to highlight that phase and coherence between multiple control accelerometers affixed to an armature, slip table, or fixture has always existed, and that the historical approach has been to minimize any flexible modes between control accelerometers. A more modern approach is to best match the flexible modes in the laboratory to the flexible modes from the in-service environment.[5] This consideration is critical when moving from SDOF to MDOF testing.

The statistical nature of PSDs and CSDs was reviewed as a function of frequency. Three-dimensional plots were presented, consisting of histograms of all ensembles at each discrete frequency. The PSD was shown to be more Gaussian distributed in the rigid-body region. The PSD exhibited less Gaussian behavior above the first flexible mode for the data presented. The CSD phase behaves similar to the PSD with a more pronounced change in distribution above the first flexible mode. The CSD coherence behaves differently; this is expected, since coherence is bounded between zero and one. In the rigid-body region, the CSD coherence is single sided near unity, and above the first flexible mode, the CSD coherence has a much lower mean value and becomes more widely distributed. Studying all data in a cloud plot is recommended when characterizing MDOF vibration environments.

When defining MDOF vibration tests, the recommendation is to capture a large data set of in-service vibration data from all relevant operating conditions. Realistic PSD and CSD tolerances should be based on observations made about the in-service vibration data when studying a cloud plot. Furthermore, the recommended ultimate goal of the MDOF vibration test is to recreate the appropriate operational dynamics. To understand operational dynamics, the statistical nature of the PSDs and the CSDs as a function of frequency should also be understood and preserved from the in-service measured data to the laboratory test definition. Preserving this data would allow a test lab the best opportunity to recreate in-service dynamics.

Future Work

This article is intended to give readers a perspective into what an actual in-service SDM looks like. The need for a statistical analysis of the full SDM with a compact way of communicating the full SDM is recognized. A compact form for describing the full SDM cloud plot would aid in communicating the information captured in the SDM. We have alluded to spectral density matrix adjustments and qualitatively compared a previously published Monte Carlo correction technique with the eigenvalue and Cholesky correction techniques. A comparative investigation of these three techniques is needed.

References
1. Paul H. Wirsching, Thomas L. Paez, and Keith Ortiz, *Random Vibrations Theory and Practice*, John Wiley & Sons, 1995.
2. Michael T. Hale, "A 6-DOF Vibration Specification Development Methodology," *Journal of the IEST*, Vol. 54, No. 2, 2011.
3. Luke A. Martin and Shawn Schneider, "Employing Monte Carlo Techniques to Explore the Spectral Density Matrix Solution Space," SAVE 2015, Orlando, FL, October 2015.
4. Luke A. Martin and Shawn Schneider, "Spectral Density Matrix Adjustments," IEST ESTECH 2015, Danvers, MA. April 2015.
5. D. J. Ewins, "Exciting Vibrations: The Role of Testing in an Era of Supercomputers and Uncertainties." Meccanica 2016, 51: 3241-3258.
6. MIL-STD 810G Change Notice 1, *Environmental Engineering Considerations and Laboratory Tests*, Method 527, 2014.
7. Julius S.Bendat and Allan G. Piersol, *Random Data*, John Wiley & Sons, 2000. **S&V**

The author can be reached at: luke.a.martin@navy.mil.